Journal of the Korean Physical Society, Vol. 69, No. 6, September 2016, pp. 1110∼1114

Synthesis and Luminescent Properties of $Gd_3Ga_2Al_3O_{12}$ Phosphors Doped with Eu^{3+} or Ce^{3+}

M. J. Oh
Department of Physics, Kyungpook National University, Daegu 41566, Korea and
Department of Radiology, Daegu Health Colleage, Daegu 41453, Korea

H. J. Kim*
Department of Physics, Kyungpook National University, Daegu 41566, Korea

(Received 11 December 2015, in final form 10 May 2016)

Eu^{3+}-or Ce^{3+}-doped gadolinium gallium aluminum garnet (GGAG), $Gd_3Ga_2Al_3O_{12}$, phosphors are fabricated using solid-state reactions with Gd_2O_3, Ga_2O_3, Al_2O_3, CeO_2 and Eu_2O_3 powders. The Eu^{3+}-or Ce^{3+}-doped $Gd_3Ga_2Al_3O_{12}$ phosphors are sintered at 1300 °C or 1600 °C for 5 hours by using an electric furnace under normal atmosphere. X-ray diffraction and field-emission scanning electron microscopy studies are carried out in order to analyze the physical properties of these materials, and their luminescence properties are also measured by using UV and X-ray sources. The Eu^{3+}-or Ce^{3+}-doped $Gd_3Ga_2Al_3O_{12}$ phosphors show higher light yields in comparison to commercial phosphors such as Gd_2O_2S:Tb (gadox). This indicates that $Gd_3Ga_2Al_3O_{12}$:Eu^{3+} phosphors are promising materials for use in X-ray imaging and dose monitoring at proton beamlines.

PACS numbers: 29.40.Mc, 78.55.Hx, 81.05.Pj
Keywords: $Gd_3Ga_2Al_3O_{12}$, Phosphor, Eu^{3+}, Ce^{3+}
DOI: 10.3938/jkps.69.1110

I. INTRODUCTION

In recent years, phosphor materials have begun to draw more research attention due to their various potential applications in the field of medical imaging. Medical imaging techniques such as positron emission tomography (PET) and X-ray computed tomography (CT) have seen increased development since the X-ray was discovered in 1985 [1]. While BGO ($Bi_4Ge_3O_{12}$) has traditionally been one of the most effective scintillators used in medical imaging techniques, the use of garnet materials has attracted more research attention in the late 20^{th} century [1]. In particular, yttrium silicate (Y_2SiO_5:Ce) or yttrium aluminum garnet doped with Ce ($YAlO_3$:Ce) have been shown to be suitable for beam-index-type cathode-ray tubes or flying spot scanner because of the fast decay time (about 10^{-7} to 10^{-8} s) of the 5d-4f transition [1]. Numerous studies have shown that Ce-doped scintillators have various other advantages apart from this fast decay time; for example, Ce^{3+}-doped lanthanide phosphors are well known as efficient light-emitting materials because of the large energy band gap from $^5d_1$ to the nearest level ($^2F_{7/2}$ level) [1]. Thus, the Ce^{3+} ion is drawing more attention in the field of high-energy physics due to this fast decay time and efficient UV luminescence. However, commercial Y_2SiO_5:Ce^{3+} and $YAlO_3$:Ce^{3+} are low-density materials, and this low density imparts considerable defects in the X-ray and gamma-ray transmittance onto these materials. Effective phosphor have several required characteristics, such as strong X-ray absorption, high emission efficiency, short emission decay time, a match between the emission spectrum and the spectral sensitivity of the radiographic film, and the durability and dispersion of the material [2]. Continuous research is required to develop more efficient phosphor as these materials minimize the X-ray radiation exposure experienced by patients during medical imaging.

Because of the advantages stated above, rare-earth-doped phosphors are seen as attractive materials for potential use in this field. For example, a gadolinium-oxide (Gd_2O_3: 7.4 g/cm^3)-containing $Gd_3Ga_2Al_3O_{12}$ phosphor has shown excellent absorption efficiency for X-ray or gamma-ray radiation compared to other similar materials [2]. In a similar vein, the luminescence properties of Ce^{3+}-or B^{3+}-doped $Gd_3Ga_2Al_3O_{12}$ phosphors and Ce-doped $Gd_3(Ga,Al)_5O_{12}$ single crystals have also been examined [1, 3, 4]. This report, however, presents what is, to the best of our knowledge, the first study of a Eu^{3+}-doped $Gd_3Ga_2Al_3O_{12}$ phosphor. The Eu^{3+} ion is a well-known activator for commercial phosphors that emit wavelengths of approximately 600 nm (red light),

*E-mail: hongjoo@knu.ac.kr

and a number of these emission lines are caused by ^5D_j to ^7F_j transitions [6]. In a similar manner, the Ce^{3+} ion shows a dipole-allowed $5d$ to $4f$ transition energy at approximately 550 nm (yellow light). The rare-earth-doped phosphors can be used in various other industrial applications, such as in cathode-ray tubes, lamps, fluorescent displays, X-ray fluorescent screens, and luminous paints [1]. They can also be used for proton, electron and heavy-ion beam position monitoring. The aim of this study is to examine the X-ray and the UV luminescence properties of Ce-or Eu-doped gadolinium gallium aluminum garnet synthesized using solid-state reactions with Gd_2O_3, Ga_2O_3, Al_2O_3, CeO_2 and Eu_2O_3 powders.

II. EXPERIMENTAL

The Eu^{3+}-or Ce^{3+}-doped $Gd_3Ga_2Al_3O_{12}$ phosphors were synthesized using conventional solid-state reactions with a horizontal electric furnace. The starting materials were gadolinium oxide (Gd_2O_3, 99.99%), aluminum oxide (Al_2O_3, 99.99%), gallium oxide (Ga_2O_3, 99.99%), europium oxide (Eu_2O_3, 99.99%) and cerium oxide (CeO_2, 99.99%). The mixtures were blended via ball milling and sintered at 1300 and 1600 °C for 5 h, respectively, under a normal atmosphere. Powder X-ray diffraction (XRD, Panalytical X′Pert Pro) and field-emission scanning electron microscopy (FE-SEM) were performed to analyze these materials. For the XRD analysis, a Cu-Kα X-ray source was used with a scan range of 20 ∼ 80° (2θ), a scan speed of 0.02°/s, and a step size of 0.01°. The accelerating voltage and the tube current were 40 kV and 30 mA, respectively. Luminescence spectra were collected using a Xe-lamp and an X-ray source. For the photoluminescence spectra, a Fluorolog-3 spectrofluorimeter was used in conjunction with a Xe-lamp. The X-ray-excited radio-luminescence spectra were collected and analyzed with an Ocean Optics QE-65000 spectrometer. The X-ray tube current and the accelerating voltage were adjusted to 65 kV and 1 mA, respectively.

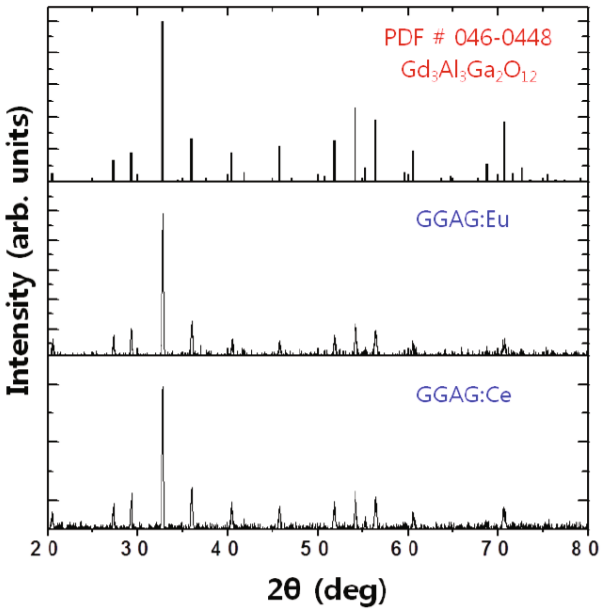

Fig. 1. (Color online) XRD patterns of Eu^{3+}-or Ce^{3+}-doped $Gd_3Ga_2Al_3O_{12}$ phosphors and of standard PDF card # 046-0448($Gd_3Ga_2Al_3O_{12}$).

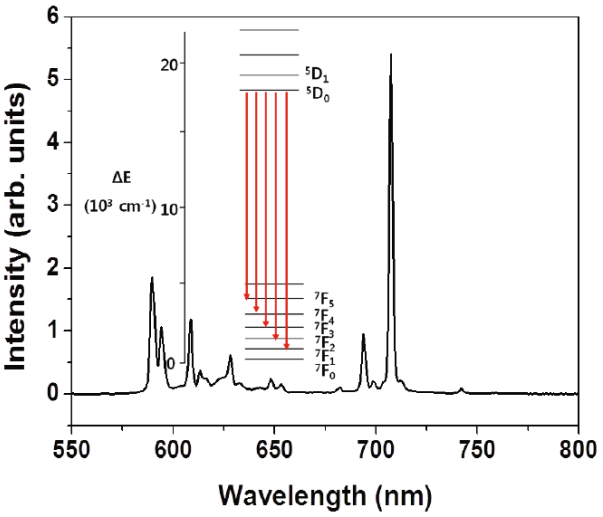

Fig. 2. (Color online) Emission spectra of the Eu^{3+} doped $Gd_3Ga_2Al_3O_{12}$ phosphors excited by X-rays.

III. RESULT AND DISCUSSION

The X-ray diffraction patterns of the $Gd_3Ga_2Al_3O_{12}$ phosphors are shown in Fig. 1. In this figure, Eu^{3+} - or Ce^{3+}-doped $Gd_3Ga_2Al_3O_{12}$ phosphors are compared with the standard spectrum (PDF # 046-0448). The results of the XRD analysis showed that no extra peaks that corresponded to the starting materials, and all the patterns were in agreement with the reference PDF data.

Figure 2 shows the X-ray-excited luminescence spectrum of the Eu^{3+}-doped $Gd_3Ga_2Al_3O_{12}$ phosphors. The emission spectrum of the $Gd_3Ga_2Al_3O_{12}$:Eu^{3+} phosphor shows ^5D_j to ^7F_j transitions. Among these sharp peaks, the strongest peak is observed at 708 nm due to the ^5D_o to $^7F_4$ transitions. Others are observed at 590 and 594 nm due to the ^5D_o to $^7F_1$ transition, at 608, 613 and 628 nm due to the ^5D_o to $^7F_2$ transition, at 648 and 653 nm due to the ^5D_o to $^7F_3$ transition, at 682, 694, 698 and 707 nm due to the ^5D_o to $^7F_4$ transition and at 742 nm due to the ^5D_o to $^7F_5$ transition [6–9].

The photoluminescence emission and excitation spectra of the Eu^{3+} -doped $Gd_3Ga_2Al_3O_{12}$ phosphor are shown in Fig. 3, and the X-ray-excited radio-luminescence and UV-excited photoluminescence are compared to each other. While the wavelengths of the emission peaks are coincident for the radio-luminescence

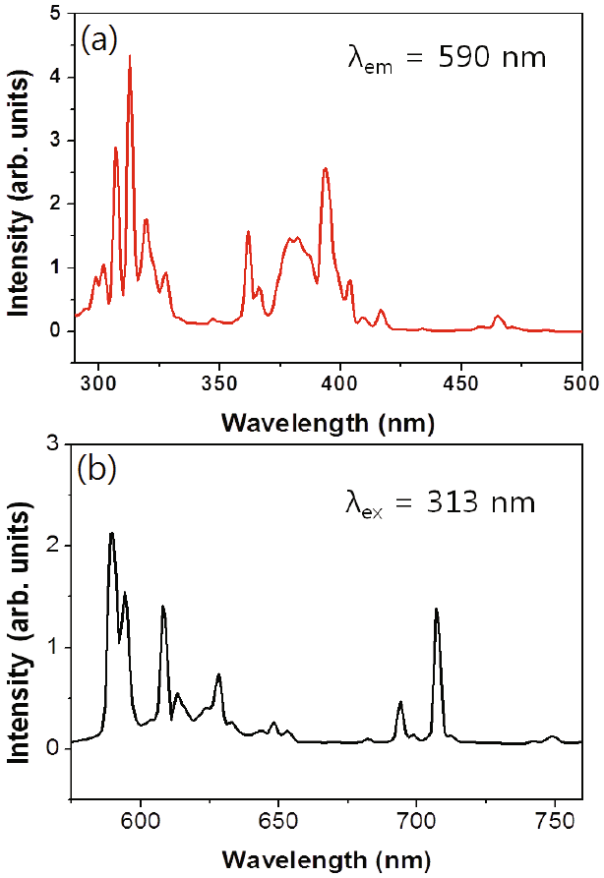

Fig. 3. (Color online) Photoluminescence (a) excitation and (b) emission spectra of the $Gd_3Ga_2Al_3O_{12}$:Eu^{3+} phosphor.

and the photoluminescence observations, the intensities of the luminescence peaks do not corresponded exactly to each other. The UV-excited emission spectrum, Fig. 3(b), shows several sharp peaks that arise from different $^5D_0$ to ^7F_j transitions, the strongest of which is due to the $^5D_0$ to $^7F_1$ transition at 590 nm. Other incident peaks from the $^5D_0$ to $^7F_2$ transition are observed at 608, 613 and 628 nm, these from the $^5D_0$ to $^7F_3$ transition are observed at 648 & 653 nm, and these from the $^5D_0$ to $^7F_4$ transition are observed at 694 and 707 nm. The excitation spectrum, Fig. 2(a) at a wavelength of 590 nm shows sharp peaks and broad bands, the strongest of which is located at 313 nm (associated with the $^7F_0$ to ^5H_j transition). Others occur at 299 nm ($^7F_0$ to $^5F_4$), 302 and 307 nm ($^7F_0$ to $^5F_{2-3}$), 320 and 327 nm ($^7F_{0,1}$to ^5H_j), 362 and 366 nm ($^7F_{0,1}$ to $^5D_4$), 380 nm ($^7F_{0,1}$ to ^5G_j), 393 and 404 nm ($^7F_{0,1}$ to $^5L_6$), 410 and 416 nm ($^7F_{0,1}$ to $^5D_3$), and 465 nm ($^7F_{0,1}$ to $^5D_2$) [6–9,11,12].

The X-ray-excited luminescence spectrum of the Ce^{3+}-doped $Gd_3Ga_2Al_3O_{12}$ phosphor is shown in Fig. 4, where the characteristic emission band of the Ce^{3+} 5d-4f transition is observed between 500 and 750 nm [15]. The broad band of the Ce^{3+}-doped $Gd_3Ga_2Al_3O_{12}$ phosphor, as caused by using 454 nm-excitation, is also shown in

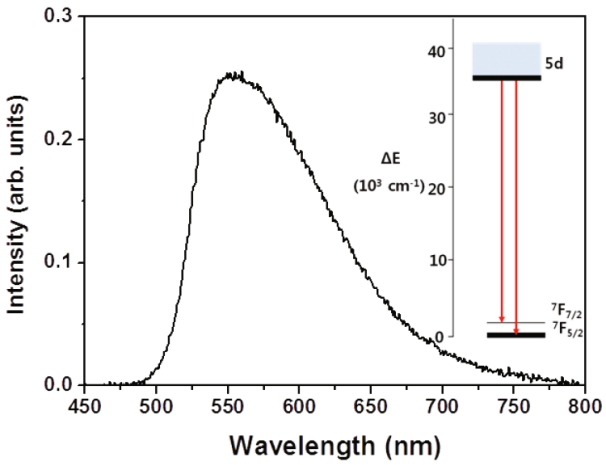

Fig. 4. (Color online) Emission spectra of the Ce^{3+}-doped $Gd_3Ga_2Al_3O_{12}$ phosphors excited by X-rays.

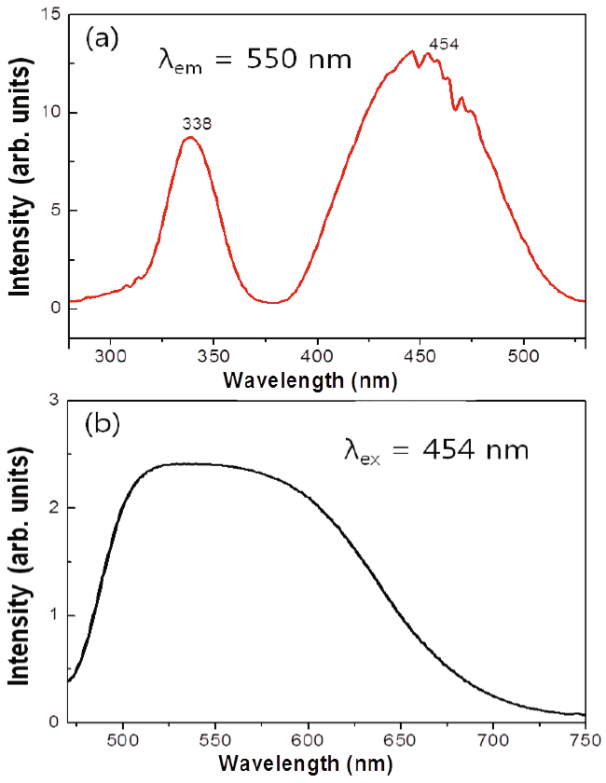

Fig. 5. (Color online) Photoluminescence (a) excitation and (b) emission spectra of the $Gd_3Ga_2Al_3O_{12}$:Ce^{3+} phosphor.

Fig. 5(b). Figure 5 shows the emission and the excitation spectra of Ce^{3+}-doped $Gd_3Ga_2Al_3O_{12}$ phosphor as induced by UV radiation. The ground state of Ce^{3+} shows two spin-orbital splitting energy levels corresponding to $^2F_{5/2}$ and $^2F_{7/2}$ [1,5,10,13–15]. The UV excitation spectrum, Fig. 5(a) from the 550 nm excitation shows two broad bands, 320 to 360 nm (UV light) and 400 to 500

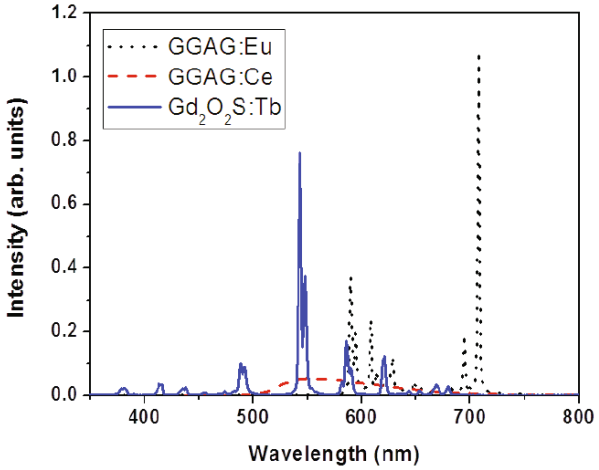

Fig. 6. (Color online) Relative light yields of Eu^{3+}-or Ce^{3+}-doped $Gd_3Ga_2Al_3O_{12}$ phosphors compared with that of commercial Gd_2O_2S:Tb.

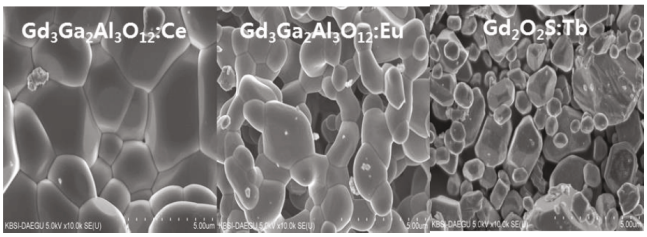

Fig. 7. FE-SEM images of Eu^{3+}-or Ce^{3+}-doped $Gd_3Ga_2Al_3O_{12}$ phosphors and the Gd_2O_2S:Tb phosphor (gadox).

nm (blue light), due to $^2F_{5/2}$ and $^2F_{7/2}$ to ^5D states, respectively. The energy gap from $^5D_1$ to $^2F_{7/2}$ is so large that the 5d state offers efficient light emission [1].

In X-ray imaging fields, efficient light yield is the most important property for an imaging agent. Figure 6 shows the relative light yield of the Eu^{3+}-or Ce^{3+}-doped $Gd_3Ga_2Al_3O_{12}$ phosphors compared to relative light yield of commercial Gd_2O_2S:Tb (gadox); this material is widely used as a green phosphor in projection CRTs and as a scintillator for X-ray imaging detectors in medical diagnostics because of the high density (7.34 g/cm^3) of Gd_2O_2S:Tb [16,17]. Eu^{3+}-or Ce^{3+}-activated $Gd_3Ga_2Al_3O_{12}$ phosphors show 127% and 89% light yields in comparison to Gd_2O_2S:Tb, respectively, demonstrating that Eu^{3+} activated $Gd_3Ga_2Al_3O_{12}$ phosphor is better than commercialized Gd_2O_2S:Tb in terms of light yield efficiency. FE-SEM images of these materials are presented Fig. 7, comparing the Eu^{3+}-or Ce^{3+}-activated $Gd_3Ga_2Al_3O_{12}$ phosphors with Gd_2O_2S:Tb. These images show the grain size and the grain shape of the phosphors on a scale of 5 μm while the grain sizes of the Gd_2O_2S:Tb phosphor and the Eu^{3+}-or Ce^{3+}-activated $Gd_3Ga_2Al_3O_{12}$ phosphors are measured on a much larger scale.

IV. CONCLUSIONS

In this research, we studied the optical properties of Eu^{3+}-or Ce^{3+}-activated $Gd_3Ga_2Al_3O_{12}$ phosphors, and to our knowledge, this is the first time such a study has been carried out on an Eu^{3+}-activated $Gd_3Ga_2Al_3O_{12}$ phosphor. The UV-excited photoluminescence and X-ray-excited radio-luminescence were compared to each other. The $Gd_3Ga_2Al_3O_{12}$:Eu^{3+} phosphor shows ^5D_j to ^7F_j transitions at approximately 550 to 750 nm. The wavelengths of the red region are well matched with the quantum efficiency of the typical charge coupled device (CCD), and the Ce^{3+}-doped $Gd_3Ga_2Al_3O_{12}$ phosphor shows yellow luminescence between 500 and 750 nm due to the $5d-4f$ transition [17]. The relative light yield was measured and compared to that of commercially-available gadox (Gd_2O_2S:Tb). For a more detailed comparison between gadox and the fabricated phosphors, the grain size was measured as it has a strong influence on the light yield of the material [17], the Eu^{3+}-activated $Gd_3Ga_2Al_3O_{12}$ phosphors were found to show greater light efficiency than the Gd_2O_2S:Tb. This indicates that the Eu^{3+}-activated $Gd_3Ga_2Al_3O_{12}$ phosphor is a promising material for X-ray imaging and beam position monitoring at the beamline.

ACKNOWLEDGMENTS

These investigations were supported by the Technology Innovation Program (No. 10049569) funded by the Ministry of Trade, industry & Energy (Mi, Korea).

REFERENCES

[1] J. M. Ogiegło, A. Katelnikovas, A. Zych, T. Jüstel, A. Meijerink and C. R. Ronda, J. Phys. Chem. A **117**, 2479 (2013).
[2] G. F. Knoll, *Radiation Detection and Measurement* (John Wiley & Sons, Inc., New York, 1979).
[3] J. G. Kang, M. K. Kim and K. B. Kim, J. Mate. Res. Bull. **43**, 1982 (2008).
[4] K. Kamada, T. Yanagida, J. Pejchal, M. Nikl, T. Endo, K. Tsutsumi, Y. Fujimoto and A. Fukabori, *et al.*, IEEE Trans. Nucl. Sci. **59**, 2112 (2012).
[5] W. M. Yen, S. Shionoya and H. Yamamoto, *Practical applications of phosphors* (CRC Press Taylor & Francis Group, New York, 2007).
[6] M. J. Oh, H. J. Kim, Fawad. U, H. Park and S. H. Kim, IEEE Trans. Nucl. Sci. **60**, 1006 (2013).
[7] M. Karbowiak, E. Zych and J. Holsa, J. Phys. Condens. Matter **15**. 2169 (2003).
[8] Y.-C. Li, Y.-H. Changa, Y.-F. Lin, Y.-S. Chang and Y.-J. Lin, J. Alloy and Comp. **439**, 367 (2007).
[9] Lj. R. Dacanin, M. D. Dramicanin, S. R. Lukic-Petrovic, D. M. Petrovic and M. G. Nikolic, Rad. Measure. **56**, 143 (2013).

[10] B. Dhabekar, E. Alague Raja, S. Menon, T. K. Gundu Rao, R. K. Kher and B. C Bhatt, Rad. Measure. **43**, 291 (2008).
[11] F. F. da Silva, F. L. de Menezes, L. L. da Luz and S. Alves, J. Chem. **38**, 893 (2014).
[12] G. Ju, Y. Hu, H. Wu, Z. Yang, C. Fu and F. Kang, Opt. Materi. **33**, 1297 (2011).
[13] B. Huang, Y. Ma, S. Qian, G. Zhenf and Z. Dai, Opt. Materi. **36**, 1561 (2014).
[14] K. V. Ivanovskikh, J. M. Ogiegto, C. R. Ronda and A. Meijerink, J. Solid State Sci. Techn. **2**, 3148 (2013).
[15] T. Kärner, V. V. Laguta, M. Nikl, T. Shalapska and S. Zazubovich, J. Phys. D **47**, 065303 (2014).
[16] E.-J. Popovici, L. Nuresan, A. Hristea-Simoc, E. Indra, M. Vasilescu, M. Nazarov and D. Y. Jeon, Opt. Materi. **27**, 559 (2004).
[17] M. Oh, H. J. Kim, S. Kim and C. Cheon, J. Korean Phys. Soc. **61**, 273 (2012).